

# Preparation and Characterization of Magnetic Polyimide Hybrid Thin Films

Jiuli Sun, Qiuyu Zhang, Feige Guo, Junwei Gu, Junping Zhang

Department of Applied Chemistry, Northwestern Polytechnical University, Xi'an 710072, China

Received 22 July 2010; accepted 3 August 2011

DOI 10.1002/app.35412

Published online 27 December 2011 in Wiley Online Library (wileyonlinelibrary.com).

**ABSTRACT:** Magnetic polyimide hybrid thin films were synthesized from pyromellitic dianhydride (PMDA), 4,4'-oxydianiline (ODA), and Fe<sub>3</sub>O<sub>4</sub> magnetic nanoparticles via thermal imidiazation in nitrogen environments. The magnetic polyimide hybrid thin films were analyzed and characterized by Fourier transform infrared spectroscopy (FTIR), X-ray diffraction (XRD), and scanning electron microscopy (SEM). The magnetic properties of magnetic nanoparticles and polymer hybrid thin films were assessed

using a vibrating sample magnetometer (VSM), and the physical properties of hybrid thin films were tested. Results revealed that the magnetic polyimide hybrid thin films had superparamagnetic behavior and excellent mechanical properties. © 2011 Wiley Periodicals, Inc. *J Appl Polym Sci* 125: 725–730, 2012

**Key words:** polyimide; hybrid films; magnetic nanocomposite

## INTRODUCTION

In recent years, hybrid organic-inorganic materials could achieve intermolecular bonding of the organic components and inorganic components, and have been widely used in coatings, films, nanocomposites, glass, and organic ceramics and other fields.<sup>1–3</sup>

Polyimides are a new type of engineering plastics. The polyimide possess excellent properties such as unmatched heat resistance, low temperature resistance, radiation resistance, excellent dielectric properties, chemical properties of stability, strong anticreep capability, and excellent friction properties.<sup>4–6</sup> The magnetic polyimide hybrid thin films have attracted considerable attention. Different magnetic polyimide nanocomposites have been prepared, which show low coefficient of thermal expansion (CTE) and excellent mechanical property.<sup>7–13</sup> However, the content of nanoparticles is very low in the polymer composites. In addition, the superparamagnetic behavior of the polyimide nanocomposites is seldom reported.

In this article, novel magnetic polyimide hybrid thin films were synthesized from pyromellitic dianhydride (PMDA), 4,4'-oxydianiline (ODA), and Fe<sub>3</sub>O<sub>4</sub> magnetic nanoparticles via thermal imidiazation in nitrogen environments. The magnetic polyimide hybrid thin films were analyzed and characterized by Fourier transform infrared spectroscopy

(FTIR), X-ray diffraction (XRD), and scanning electron microscopy (SEM). The magnetic properties of magnetic particles and polymer thin films were assessed using a vibrating sample magnetometer (VSM) and the physical properties of hybrid thin films were tested. Results revealed that the magnetic polyimide hybrid thin films had typical superparamagnetic behavior and excellent mechanical properties.

## EXPERIMENTAL

### Materials

Pyromellitic dianhydride (PMDA, 99%, analytical grade), and 4,4'-oxydianiline (ODA, 99%, analytical grade) were kept in a vacuum vessel for 2 h at 50°C remove water; *N,N*-dimethylacetamide (DMAC, 99.5%, analytical grade) was vacuum distilled from CaH<sub>2</sub>; sodium hydroxide (NaOH, analytical grade), ferric chloride hexahydrate (FeCl<sub>3</sub>·6H<sub>2</sub>O, analytical grade), ferrous sulfate heptahydrate (FeSO<sub>4</sub>·7H<sub>2</sub>O, analytical grade), and other reagents were used as received.

### Preparation of magnetic nanoparticle (Fe<sub>3</sub>O<sub>4</sub>)

Magnetic nanoparticles were prepared via coprecipitation of Fe<sup>3+</sup> and Fe<sup>2+</sup> ions in the presence of NaOH. Specifically, 11.2 g of FeSO<sub>4</sub>·7H<sub>2</sub>O and 16.3 g of FeCl<sub>3</sub>·6H<sub>2</sub>O were dissolved in 200 mL of deionized water in a flask. This solution was stirred, followed by adding 3M NaOH solution quickly at 30°C until the mixture reached a pH around 11. After 30 min, the mixture was then heated to 80°C for

Correspondence to: Q. Zhang (qyzhang@nwpu.edu.cn).

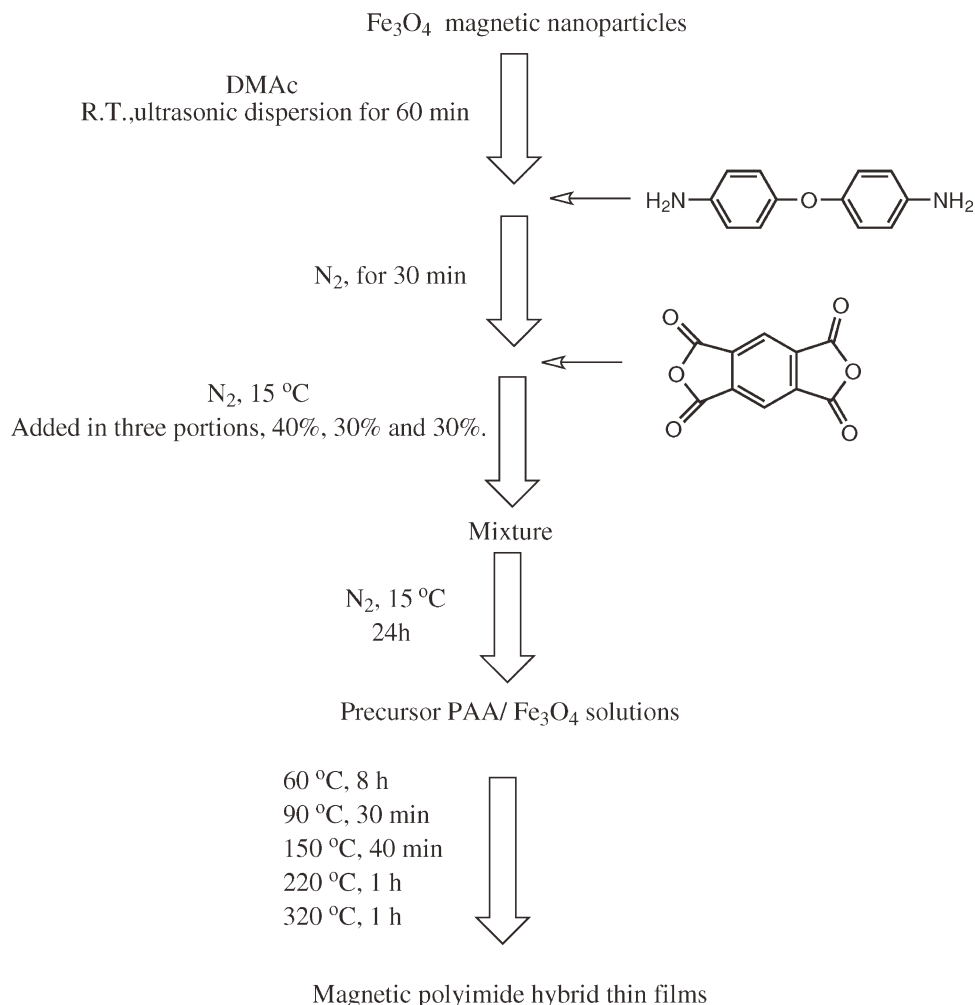


**Figure 1** Preparation route for the magnetic polyimide hybrid thin films.

30 min. The Fe<sub>3</sub>O<sub>4</sub> precipitation was isolated from the solution by magnetic separation and washed with deionized water until pH 7 was reached. Finally, the magnetic nanoparticles were sealed and stored at room temperature.<sup>14</sup>

### Preparation of magnetic polyimide hybrid thin films

The magnetic polyimide hybrid thin films were synthesized by PMDA and ODA with magnetic nanoparticle (Fe<sub>3</sub>O<sub>4</sub>) as shown in Figure 1.

The above magnetic Fe<sub>3</sub>O<sub>4</sub> nanoparticles were charged into the beaker containing DMAc, and then the beaker was placed in ultrasonic dispersion reactor for 60 min, Fe<sub>3</sub>O<sub>4</sub> nanoparticles were uniformly dispersed into DMAc. Then a 150 mL three-necked flask fitted with a stirrer, argon inlet, drying tube and stopper was purged with dry nitrogen for 30 min. Various weights of DMAc containing Fe<sub>3</sub>O<sub>4</sub> nanoparticles was charged into the reactor through an addition funnel (the amounts used were listed in the Table I). The vessel was then charged with ODA

(3.0036 g, 0.015 mol), PMDA(3.2718 g, 0.015 mol) was added to the reactor in three portions, 40%, 30% and 30%, respectively, through another addition funnel over a period of 1 h until complete dissolution of the diamines was achieved. The reaction mixture was stirred at 15°C in a dry nitrogen atmosphere resulting in a viscous polyamic acid (PAA) solution containing Fe<sub>3</sub>O<sub>4</sub> nanoparticles after 24 h. The precursor solutions may be stored in dry bottles at -5°C under nitrogen atmosphere.<sup>15</sup>

The precursor PAA/Fe<sub>3</sub>O<sub>4</sub> solutions were cast onto a clean glass substrate using a hand-coater system.

**TABLE I**  
Monomer Compositions Used for Magnetic Polyimide Hybrid Films Synthesis

Polymer code	PMDA (mol)	ODA (mol)	Magnetic nanoparticle (Fe <sub>3</sub> O <sub>4</sub> ) (wt %)
PI <sub>0</sub>	0.015	0.015	0
PI <sub>1</sub>	0.015	0.015	1
PI <sub>2</sub>	0.015	0.015	5
PI <sub>3</sub>	0.015	0.015	8

The PAA/Fe<sub>3</sub>O<sub>4</sub> nanocomposite films were heated at 60°C in a forced air for 8 h to move most of the solvent. Then they were imidized with a heating program of 90°C for 30 min, then 150°C for 40 min, 220°C for 1 h, and 320°C for 1 h in nitrogen environments. The films were then cooled to room temperature, soaked in water, and stripped from the plates. After drying the films at 120°C for 4 h in vacuum, the light-yellow PI<sub>0</sub> and magnetic polyimide hybrid thin films denoted PI<sub>1-3</sub> in Table I were obtained.

### Analysis and characterization

Fourier transform infrared spectroscopy (FTIR) was acquired on a TENSOR27 FTIR spectrometer (Bruker). The samples were prepared by mixing composite microspheres with KBr and pressing into a compact pellet.

The microscopic morphologies of Fe<sub>3</sub>O<sub>4</sub> particles were observed in a transmission electron microscope (TEM, JEOL JEM-3010).

The fractured surface morphology of tensile tested specimens and the surface structure of the prepared composites were examined with a scanning electron microscope (SEM), JEOL JSM 6700 at an accelerating voltage of 10 kV. Prior to examination, the surface of the specimen was coated with a thin layer of gold.

X-ray diffraction profiles were detected using Cu K $\alpha$  radiation, generated with XRD-7000 (Shimadzu limited) at 40 kV, 40 mA. The patterns were recorded from 5° to 80° (2 $\theta$  value) with a scanning rate of 10°/min.

The magnetic properties of magnetic particles and polymer thin films were assessed using a vibrating sample magnetometer (VSM, LakeShore 7307).

The mechanical properties (modulus, tensile strength, and elongation at break) of polyimide hybrid films were determined using Electron

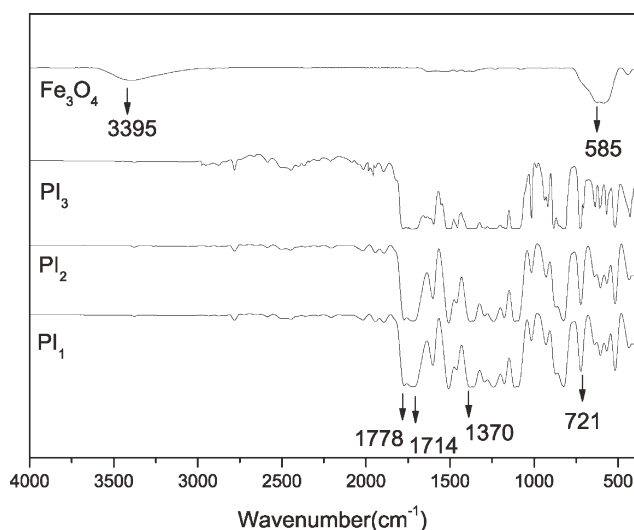


**Figure 2** Infrared spectra of Fe<sub>3</sub>O<sub>4</sub> and magnetic polyimide hybrid films.

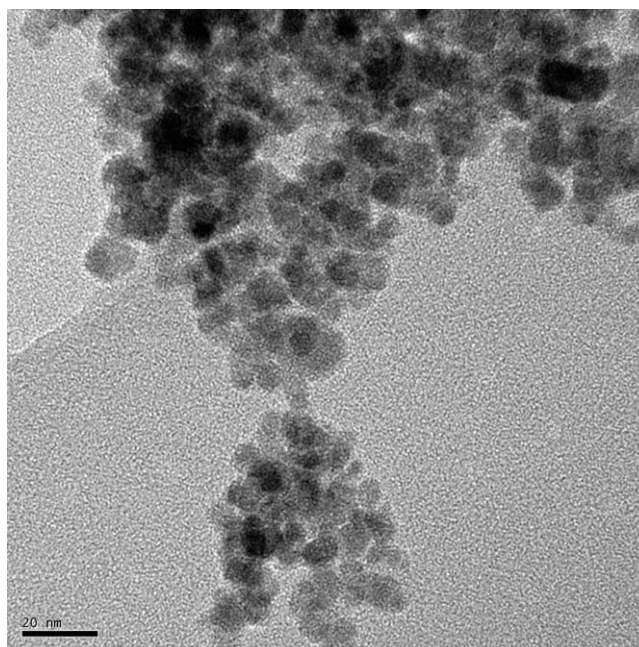


**Figure 3** The TEM images of Fe<sub>3</sub>O<sub>4</sub> nanoparticles.

Omnipotence Experiment Machine SANS-CMT5105 (Shenzhen New Sansi Corp., China) according to standard GB/T13541-92. The films were cut into strips of 15 mm × 200 mm in size. Samples were carried out at a cross-head speed of 10 mm/min.

## RESULTS AND DISCUSSION

### Characterizations of magnetic Fe<sub>3</sub>O<sub>4</sub> nanoparticles and polyimide hybrid films

Figure 2 shows the FTIR spectra of Fe<sub>3</sub>O<sub>4</sub> nanoparticles and magnetic polyimide hybrid films. In Figure 2, the characteristic absorption band of Fe<sub>3</sub>O<sub>4</sub> appears at 585 cm<sup>-1</sup>. The broad band centered at around 3395 cm<sup>-1</sup> is assigned to the OH, which is attributed to residual water on the surface of Fe<sub>3</sub>O<sub>4</sub> nanoparticles. While in Figure 2 of magnetic polyimide, the two absorption bands mentioned above almost disappeared, and many characteristic absorption bands of polyimide occur. Where the characteristic imide group absorptions at 1778 and 1714 cm<sup>-1</sup> (imide carbonyl asymmetrical and symmetrical stretching), at 1370 cm<sup>-1</sup> (C–N stretching), and at 721 cm<sup>-1</sup> (C–N bending) were evident.<sup>16,17</sup> The characteristic absorption of the amide carbonyl at 1650 cm<sup>-1</sup> did not appear in the spectrum of the imidize sample, which revealed that the imidization reaction was complete.

Figure 3 shows the TEM images of Fe<sub>3</sub>O<sub>4</sub> nanoparticles. As shown in Figure 3, the Fe<sub>3</sub>O<sub>4</sub> nanoparticles are aggregated because of their very small average particle size of around 10 nm.

Figure 4 shows the SEM images surface (a) and fractured surface (b) of magnetic polyimide hybrid

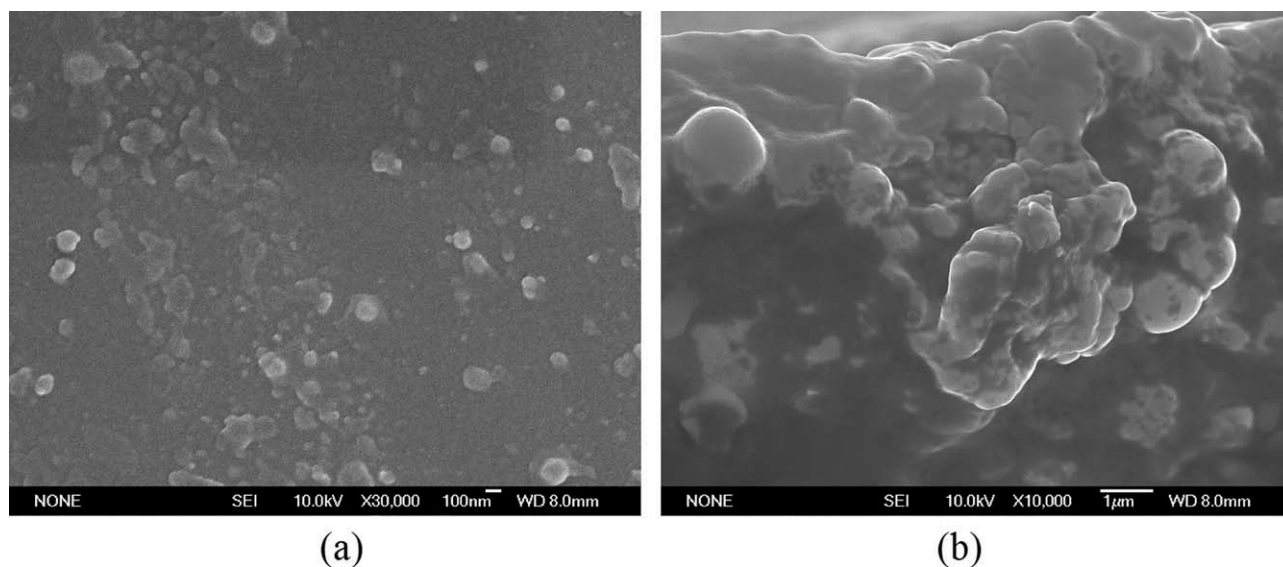


**Figure 4** The SEM images surface (a) and fractured surface (b) of magnetic polyimide hybrid films (5 wt %).

films (5 wt %  $\text{Fe}_3\text{O}_4$ ). As shown in Figure 4, the average particle size of magnetic nanoparticles dispersed in polyimide matrix is about 400 nm. So nanoparticles have quite extent reunion phenomenon.

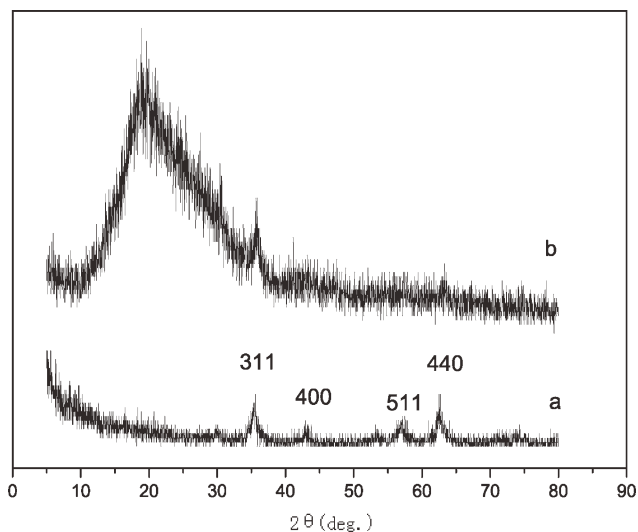
Figure 5 shows the X-ray diffraction patterns for  $\text{Fe}_3\text{O}_4$  (a) and magnetic polyimide hybrid films (5 wt %  $\text{Fe}_3\text{O}_4$ ) (b). Typical diffraction pattern for  $\text{Fe}_3\text{O}_4$  nanoparticles is shown in Figure 5(a), the peaks of  $\text{Fe}_3\text{O}_4$  nanoparticles at  $2\theta = 35.481^\circ$ ,  $43.307^\circ$ ,  $56.864^\circ$ , and  $62.495^\circ$  correspond to (311), (400), (511), and (440) Bragg reflection.<sup>18,19</sup> Figure 5(b) shows the X-ray diffraction patterns of magnetic polyimide hybrid films (5 wt %  $\text{Fe}_3\text{O}_4$ ). The characteristic peaks of  $\text{Fe}_3\text{O}_4$  nanoparticles weakened and the low intensity peaks were not observed because the percentage of magnetic nanoparticles is very low.

Magnetic response is a fundamental property of magnetic materials.<sup>20</sup> The magnetic hysteresis loop characterizes the response ability (magnetization,  $M$ ) of magnetic materials to an external magnetic field (denoted by the magnetic field strength,  $H$ ). It can provide the major magnetic parameters of magnetic materials, that is, saturation magnetization ( $M_s$ , it reflects the magnetizability of magnetic materials), coercive force ( $H_c$ , it characterizes the ability of magnetic materials to retain magnetization when the external magnetic field is removed), and magnetic remanence ( $M_r$ , it reflects the remaining magnetization of magnetic materials when an external magnetic field is removed). Figure 6 gives the magnetic hysteresis loop of  $\text{Fe}_3\text{O}_4$  and magnetic polyimide hybrid films PI<sub>1</sub> (b), PI<sub>2</sub> (c), PI<sub>3</sub> (d).

The magnetic parameters of samples are collected in Table II. As shown in Table II, in the case of  $\text{Fe}_3\text{O}_4$  nanoparticles, a value of saturation magnetiza-

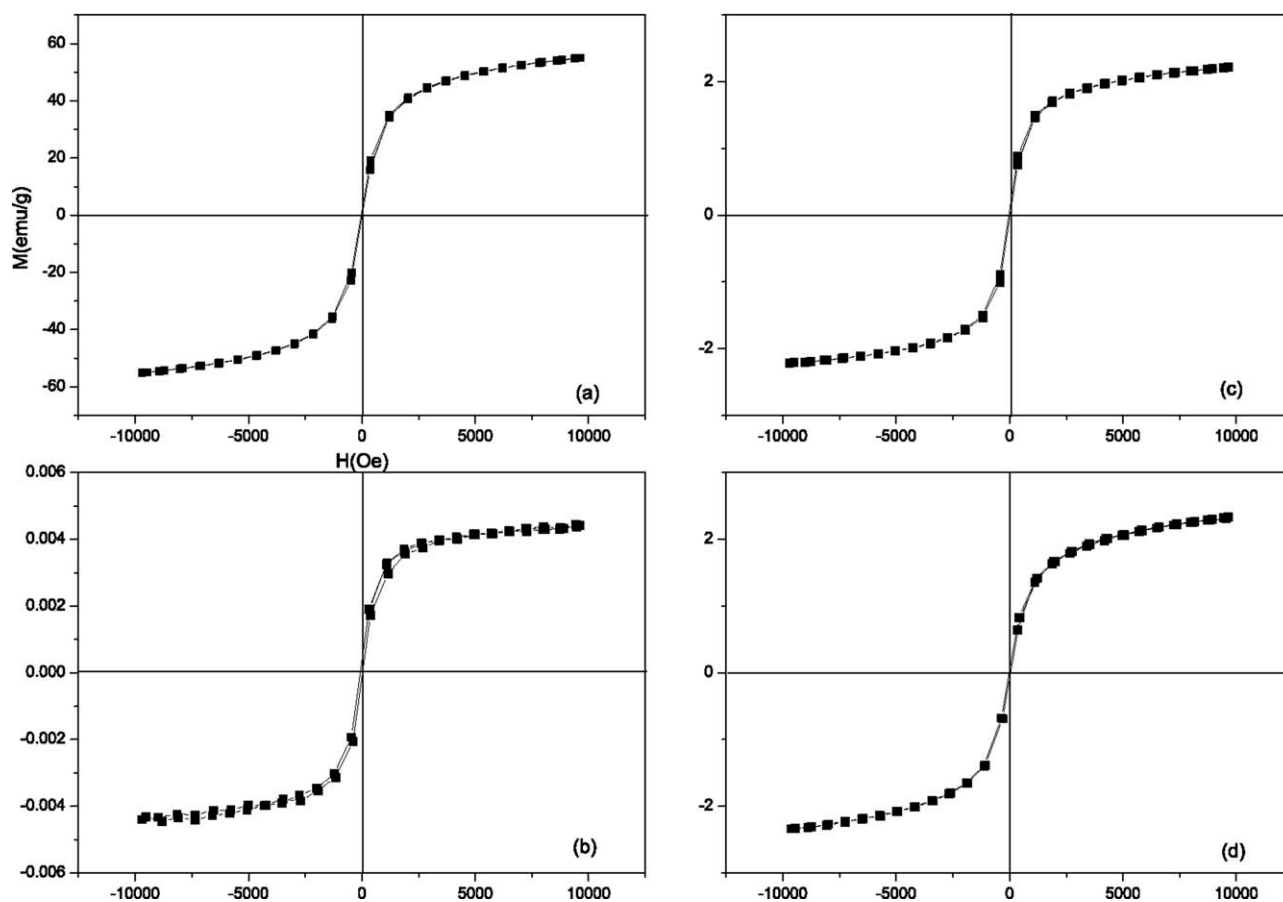
tion of 55.046 emu/g was determined. However, the saturation magnetization of the magnetic polyimide hybrid films was found to be from  $4.443 \times 10^{-3}$  emu/g to 2.336 emu/g. This can be explained by containing the nonmagnetic polymer on the magnetic composite. The saturation magnetization of the PI<sub>1</sub> magnetic polyimide hybrid film was too low, and this may be caused by instrument measurement error because of low  $\text{Fe}_3\text{O}_4$  content. In addition, the small residual magnetism and coercive force suggest that the magnetic polyimide hybrid films possess superparamagnetism as shown in Figure 6 and Table II.

Table III shows the mechanical properties of the magnetic polyimide hybrid films at room



**Figure 5** X-ray diffraction patterns for  $\text{Fe}_3\text{O}_4$  (a) and magnetic polyimide hybrid films (5 wt %) (b).





**Figure 6** The magnetization curves measured at room temperature for  $\text{Fe}_3\text{O}_4$  nanoparticles (a) and magnetic polyimide hybrid films PI1 (b), PI2 (c), and PI3 (d).

temperature. The mechanical properties of composite films are very important for their practical applications. Table III summarized the tensile properties of polyimide films obtained from the stress-strain curves. The introduction of magnetic  $\text{Fe}_3\text{O}_4$  nanoparticles caused the tensile strength to decrease from 132 MPa to 104 MPa. When the content of magnetic nanoparticles was lower, the changes of magnetic polyimide hybrid films characteristics were not more significant. Specially, the tensile properties of PI<sub>1</sub> changed well, possibly because of low content of nanoparticles that are uniformly dispersed. But the effects of characteristics became obvious when magnetic nanoparticles content increased. The elongation at break of polymer hybrid films decreased with the increasing content of nanoparticles. The polymer

became rigid and the modulus (from 2.32 GPa to 2.97 GPa) increased as the content of magnetic nanoparticles increased.

## CONCLUSIONS

In this article, the magnetic polyimide hybrid thin films were synthesized by means of direct dispersion method. The structure of polymer nanocompositions was analyzed, at the same time, magnetic and mechanical properties of materials were investigated. The study on the polyimide hybrid thin films shows that the compositions have typical superparamagnetic behavior and excellent mechanical properties.

**TABLE II**  
The Magnetic Parameters of  $\text{Fe}_3\text{O}_4$  Nanoparticles and Magnetic Polyimide Hybrid Films

Sample	$M_s$ (emu/g)	$M_r$ (emu/g)	$H_c$ (Oe)
$\text{Fe}_3\text{O}_4$ nanoparticles	55.046	1.144	24.4
PI <sub>1</sub>	$4.443 \times 10^{-3}$	$2.398 \times 10^{-4}$	48.2
PI <sub>2</sub>	2.217	$5.996 \times 10^{-2}$	26.0
PI <sub>3</sub>	2.336	$5.953 \times 10^{-2}$	30.3

**TABLE III**  
Mechanical Properties of the Magnetic Polyimide Hybrid Films

Polymer code	Tensile strength (MPa)	Elongation at break (%)	Initial modulus (GPa)	Film properties
PI <sub>0</sub>	132	23	2.32	Flexible
PI <sub>1</sub>	135	23	2.42	Flexible
PI <sub>2</sub>	121	14	2.64	Flexible
PI <sub>3</sub>	104	8.5	2.97	Flexible

## References

1. Ogoshi, T.; Itoh, H.; Kim, K. M. *Macromolecules* 2002, 35, 334.
2. Gu, J. W.; Zhang, Q. Y.; Li, H. C.; Tang, Y. S.; Kong, J.; Dang, J. *Polym Plast Technol Eng* 2007, 46, 1129.
3. Kim, K. M.; Chujo, Y. *J Mater Chem* 2003, 13, 1384.
4. Liu, X. L.; Liu, X. B. *Polym Mater Sci Eng* 2004, 20, 28.
5. Wei, M. L.; Teng, X. H.; Zhao, X. B.; Li, G. J. *Adv Ceram* 2005, 01, 15.
6. Ni, K. F.; Shan, G. R.; Weng, Z. X. *Chin Polym Bull* 2006, 11, 58.
7. Parvin, K.; Ma, J.; Ly, J.; Sun, X. C.; Nikles, D. E.; Sun, K.; Wang, L. M. *J Appl Phys* 2004, 95, 7121.
8. Brydson, J. A. *Plastics Materials*, 7th ed.; Butterworth-Heinemann: Boston, MA, 1999.
9. Ban, S.; Korenivski, V. *J Appl Phys* 2006, 99, 08R907.
10. Lee, H.; Lee, E.; Kim, D. K.; Jang, N. K.; Jeong, Y. Y.; Jon, S. *J Am Chem Soc* 2006, 128, 7383.
11. Govindaraj, B.; Sastry, N. V.; Venkataraman, A. *J Appl Polym Sci* 2004, 93, 778.
12. Lim, S. K.; Chung, K. J.; Kim, Y. H.; Kim, C. K.; Yoon, C. S. *J Colloid Interface Sci* 2004, 273, 517.
13. Kim, S. W.; Yoon, C. S. *J Magn Magn Mater* 2007, 316, e893.
14. Guo, F. G.; Zhang, Q. Y.; Zhang, B. L.; Zhang, H. P.; Zhang, L. *Polymer* 2009, 50, 1887.
15. Echigo, Y.; Iwaya, Y.; Tomioka, I.; Furukawa, M.; Okamoto, S. *Macromolecules*, 1995, 28, 3000.
16. Chen, B. K.; Tsai, Y. J.; Tsay, S. Y. *Polym Int* 2006, 55, 93.
17. Chang, C. C.; Chen, W. C. *Chem Mater* 2002, 14, 4242.
18. Zhan, J. Y.; Tian, G. F.; Jiang, L. Z.; Wu, Z. P.; Wu, D. Z.; Yang, X. P.; Jin, R. G. *Thin Solid Films* 2008, 516, 6315.
19. Koytepe, S.; Seckin, T. *Ind Eng Chem Res* 2008, 47, 4123.
20. Kaburagi, Y.; Hishiyama, Y.; Oka, H.; Inagaki, M. *Carbon* 2001, 39, 593.